

# Multiobjective Optimization of a Hydrodesulfurization Process of Diesel Using Distillation with Side Reactor

Erick Yair Miranda-Galindo,<sup>†</sup> Juan Gabriel Segovia-Hernández,<sup>\*,†</sup> Salvador Hernández,<sup>†</sup> and Adrián Bonilla-Petriciolet<sup>‡</sup>

<sup>†</sup>Departamento de Ingeniería Química, División de Ciencias Naturales y Exactas, Universidad de Guanajuato, Campus Guanajuato, Noria Alta S/N, Guanajuato Gto., 36050, Mexico

<sup>‡</sup>Departamento de Ingeniería Química, Instituto Tecnológico de Aguascalientes, Aguascalientes 20256, México

**ABSTRACT:** The distillation with side reactor has been proposed to remove sulfur compounds of diesel. The design and optimization of a hydrodesulfurization process involve the selection of the configuration and the operating conditions to minimize the total annual cost, CO<sub>2</sub> emissions, and the amount of sulfur compounds. In general, the optimal design of a hydrodesulfurization process is a nonlinear and multivariable multiobjective optimization problem, with the presence of both continuous and discrete design variables. In particular, stochastic multiobjective optimization algorithms are capable of solving, robustly and efficiently, challenging optimization problems, and they appear to be a suitable alternative for the design and optimization of complex process schemes. In this study, we have performed the multiobjective optimization of five configurations of distillation with a side reactor for the hydrodesulfurization process including an alternative using reactive distillation. The multiobjective optimization problem can be stated as a minimization of total annual cost (TAC), CO<sub>2</sub> emissions, and amount of sulfur compounds. The results obtained in the Pareto fronts indicated competition between total annual cost, CO<sub>2</sub> emissions, and the amount of sulfur compounds of the hydrodesulfurization process. These Pareto solutions are useful to identify proper conditions for the operation of this process. In general, the reduction of the amount of sulfur compounds increases the TAC and CO<sub>2</sub> emissions. However, we can identify operating conditions where the TAC can be reduced.

## 1. INTRODUCTION

Sulfur is present in many forms in petroleum fractions: mercaptans R-SH, sulfides R-S-R', disulfides R-S-S-R, polysulfides R-S<sub>n</sub>-R', thiophene, benzothiophene (BT), dibenzothiophene (DBT), and their alkyl derivatives. In addition, various nitrogen-containing components like pyridine and alkylpyridines, quinoline and alkylquinolines, benzoquinolines, acridines, indoles, and carbazoles are also present.<sup>1</sup> Sulfur has to be removed from oil fractions for both technical and environmental reasons. Regulations have been introduced in many countries to reduce the sulfur content in fuels, and the global trend for sulfur content in diesel fuels is toward 10–15 ppm.<sup>2</sup> Among several processes to obtain friendly fuels, hydrotreatment remains as the most important one to remove sulfur and other heteroatoms from petroleum fractions and heavy oils. This mandatory reduction is promoting changes in the oil refineries in terms of modifying the catalyst used and/or in the technology involved in the hydrodesulfurization (HDS) process.<sup>3</sup> Specifically, the diesel produced in Mexican refineries contains around 500 wppm of sulfur, and it is thought that the reduction to 50 wppm or less (deep HDS) will require a very important economical investment.<sup>4</sup> Some studies reported on the HDS using model sulfur compounds such as thiophene, BT, and DBT<sup>5,6</sup> as well as some of their alkyl substituents.<sup>7</sup> These HDSs with model sulfur compounds were always performed alone in the pure solvent. However, in practical hydrodesulfurization of diesel fuel, aromatic species as well as various types of sulfur compounds compete for the active sites on the HDS catalyst surface. Moreover, H<sub>2</sub>S and hydrocarbons produced in the early stage of desulfurization, from some

sulfur compounds with higher reactivity, probably influence HDS of less reactive sulfur compounds. Hence, the reactivities of various sulfur compounds in the diesel fuel need to be defined in the practical desulfurization process. Previous papers<sup>8,9</sup> have proposed a multistage deep HDS of diesel fuel, which can reduce the total sulfur content of product oil to less than 300 ppm without fluorescent color development. These studies found that the NiMo catalyst appeared to have higher catalytic activity for HDS in the second stage than that obtained with CoMo catalyst.

Knudsen et al.<sup>10</sup> have pointed out that there are two types of alternatives to achieve deep HDS of diesel: (1) increasing catalyst activity and (2) improving the performance of the reaction unit. In order to develop new catalysts for deep HDS, strong efforts are being devoted to establish relationships between the catalyst structure and the reactivity toward different molecules.<sup>11</sup> About the topic of new diesel fuel desulfurization catalysts with improved HDS activity and selectivity, Knudsen et al.<sup>10</sup> have reported that it is apparent that by increasing the hydrogen partial pressure and reducing the hydrogen sulfide concentration in the reaction unit would lead to increasing the sulfur elimination.

About improving the performance of the reaction process, Van Hasselt et al.<sup>12</sup> pointed out that a countercurrent operation of a trickle-bed reactor leads to a higher reduction of sulfur

**Received:** May 13, 2014

**Revised:** September 25, 2014

**Accepted:** September 30, 2014

**Published:** September 30, 2014

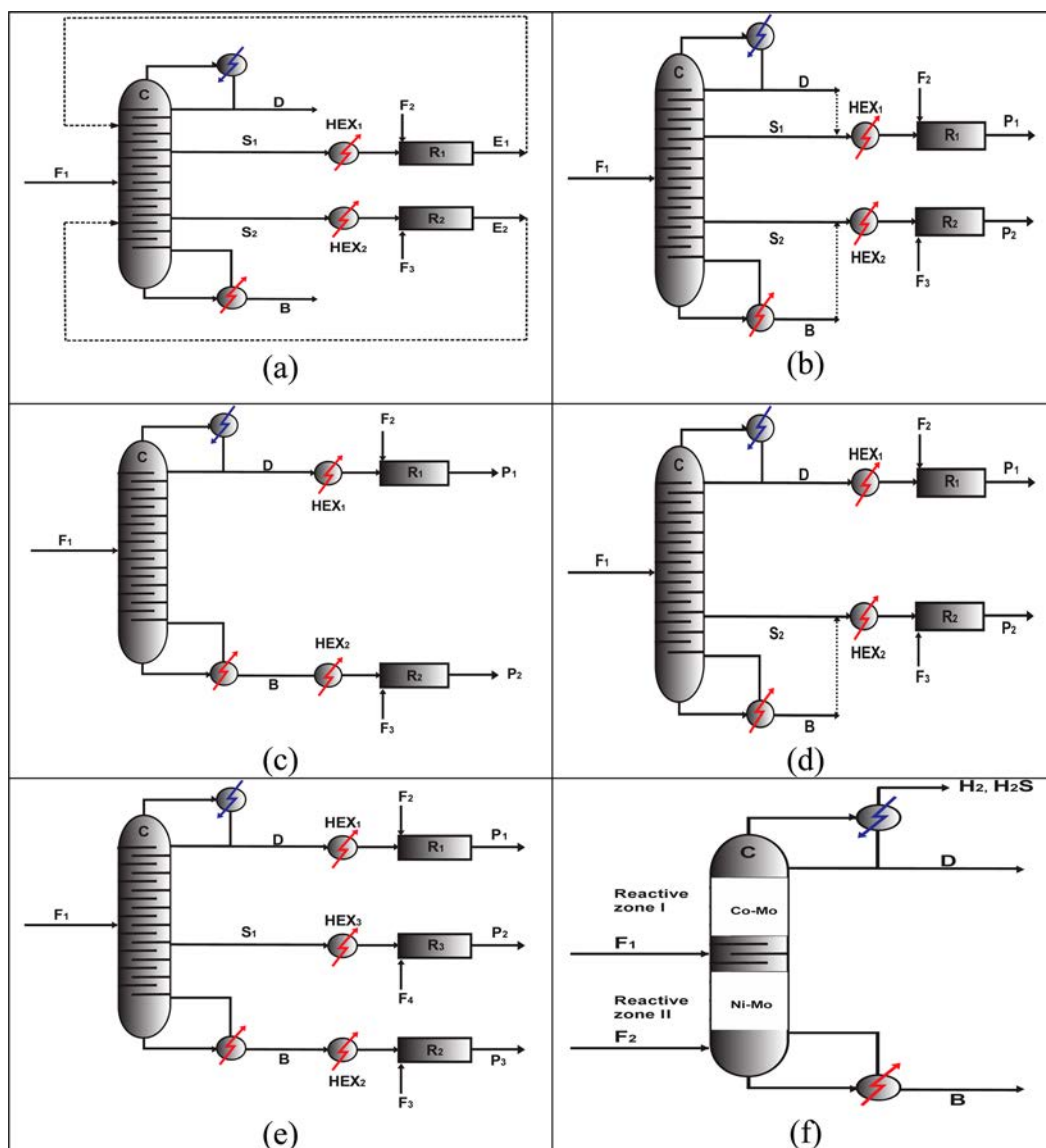


**Figure 1.** Schemes of distillation for HDS process: (a) distillation with side reactor and recirculation (DRSI), (b) distillation with side reactor and two side streams (DRSII), (c) distillation–reaction (DRI), (d) distillation with side reactor and side stream (DRSL), (e) distillation with three side reactor and side stream (DR3R), and (f) reactive distillation (RD).

content than the conventional cocurrent operation. On the other hand, only a few papers have addressed the application of reactive distillation to the deep hydrodesulfurization of diesel. Specifically, Taylor and Krishna<sup>13</sup> discussed the possibility to apply reactive distillation concepts to hydrodesulfurization of heavy oils. Hidalgo-Vivas and Towler<sup>14</sup> presented several alternative reactive distillation flowsheets to reduce the sulfur content below 500 wppm without a significant increase in process hydrogen consumption and with energy integration. However, they did not show how to apply this technology. Similarly, CdTech Company (Viveros-García et al.<sup>4</sup>) claims to have the complete development of the reactive distillation technology for ultralow sulfur diesel production, but that information is not open to the public. Viveros-García et al.<sup>4</sup> developed a conceptual design of a reactive distillation column for ultralow sulfur diesel production, which was based on a thermodynamic analysis in terms of reaction–separation feasibility. This thermodynamic analysis considers the computation of reactive and nonreactive residue curve maps for a

mixture that models the sulfured diesel fuel. Note that these authors did not carry out the design and formal optimization of synthesized arrangement. An analysis of the operating conditions to obtain ultralow sulfur diesel in a conventional HDS process suggests that reactive distillation could be an interesting technological alternative for deep HDS of diesel.<sup>4</sup> Finally, it is convenient to highlight that the design of new processes in the chemical engineering industry must take into account the policies of process intensification, which can be defined as any chemical engineering development that leads to a substantially smaller, cleaner, and more energy-efficient technology.

Traditionally, process design of separation systems is considered as a complex optimization problem due to the high nonlinearity of models used and the presence of several discrete and continuous design variables. In particular, the design of a hydrodesulfurization process can be considered as a challenging optimization problem, which may present several optimization targets. Therefore, in this paper we have used a

multiobjective optimization (MOO) approach to study and analyze the competition between total annual cost (TAC), CO<sub>2</sub> emissions, and the amount of sulfur compounds removed in the HDS process for diesel production using alternative distillation–reactor side (DRS) configurations. These process configurations were conceptually synthesized by Plaza-Rosas,<sup>15</sup> and so far, they have not been formally designed or/and optimized. In particular, we have analyzed five cases of study with different operating configurations. These process configurations are reported in Figures 1a–e. Additionally, we have compared these schemes with an HDS process based on reactive distillation (RD) as proposed by Viveros-García et al.,<sup>4</sup> see Figure 1f.

## 2. DESIGN PROBLEM STATEMENT

Feed composition (F1) is a hydrocarbon mixture of C11–C16 paraffins with four organo-sulfur compounds: thiophene (Th), benzothiophene (BT), dibenzothiophene (DBT), and 4,6-dimethyldebenzothiophene (4,6-DMDBT); see Table 1. The

**Table 1.** Feed Mixture Used in the Modeling of the HDS Process

component	formula	% mole
Th	C <sub>4</sub> H <sub>4</sub> S	0.8
BT	C <sub>8</sub> H <sub>6</sub> S	0.8
DBT	C <sub>12</sub> H <sub>8</sub> S	10
4,6-DMDBT	C <sub>14</sub> H <sub>12</sub> S	2
n-C11	C <sub>11</sub> H <sub>24</sub>	48.9
n-C12	C <sub>12</sub> H <sub>26</sub>	31.6
n-C13	C <sub>13</sub> H <sub>28</sub>	0.8
n-C14	C <sub>14</sub> H <sub>30</sub>	0.1
n-C16	C <sub>16</sub> H <sub>34</sub>	5

design targets are defined to obtain in the top of the column Th and BT, respectively, and DBT and 4,6-DMDBT in the bottom, to react with hydrogen (F2, F3). To perform the simulation of distillation process with side reactors in the HDS, it is necessary to know the kinetic expressions of sulfur compounds describing hydrodesulfurization reactions. In this work, we used the kinetic expressions reported in the literature for Th,<sup>16</sup> BT,<sup>17</sup> DBT,<sup>1</sup> and 4,6-DMDBT.<sup>18</sup> For example, there are two possible reaction paths for sulfur removal from the organo-sulfur compounds, as illustrated for dibenzothiophene in Figure 2. The first route is the sulfur atom direct extraction (i.e., hydrogenolysis) from the sulfured molecule. The second route is the hydrogenation of one aromatic ring followed by the sulfur atom extraction.

The dibenzothiophene HDS reaction progresses preferentially via the direct extraction route.<sup>10</sup> When alkyl substituents are attached to the carbon atoms adjacent to the sulfur atom, the rate for direct sulfur extraction is diminished whereas the sulfur removal rate via the hydrogenation route is relatively unaffected. Co–Mo catalysts desulfurize primarily via the direct route, while the Ni–Mo catalyst does it via the hydrogenation route. In general, the extent to which a given catalyst acts via one route or the other is determined by the H<sub>2</sub> and H<sub>2</sub>S partial pressures and feed properties, as suggested in the work of Van Parijs et al.<sup>16</sup> and other authors. Despite the fact that 80% of the HDS of 4,6-DMDBT goes by the hydrogenation route with the conventional Ni–Mo catalysts, due to the lack of thermodynamic data for this compound and the uncertainty on the predicted properties, the design was performed considering

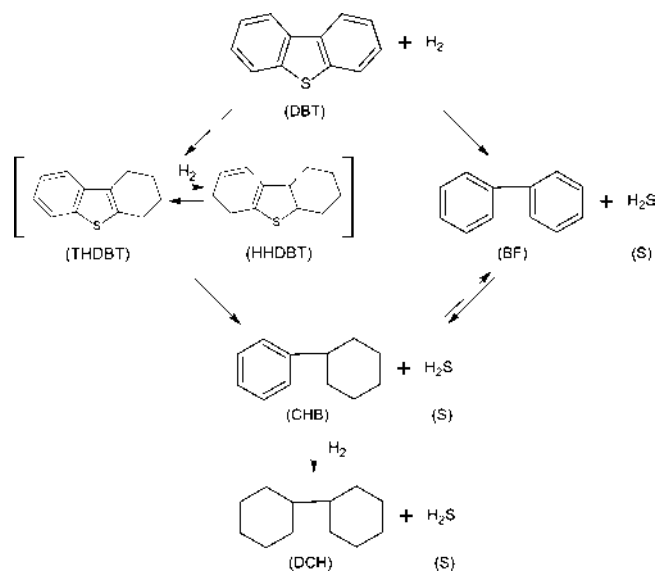


**Figure 2.** Reaction pathways for HDS of DBT.

only DBT as the sulfur compound present in the diesel.<sup>4</sup> Also, it is well-known that HDS of DBT follows preferentially the direct extraction route and, in order to simplify the design, only this reaction route (hydrogenolysis) for DBT is considered.<sup>4</sup> To carry out the modeling of the kinetics of reaction in the simulator, the model LHHW available in the Aspen Plus simulator was used. This model is consistent with the kinetics reported in the literature, and the results are consistent with those reported in industry (Viveros-García et al.<sup>4</sup>). To perform the design and optimization of the distillation column with side reactors for HDS processes, it is necessary to have the data of the physical and thermodynamic properties of the compounds present in the system. Specifically, properties of sulfur compounds and some products of the hydrogenolysis reactions are not well-known. Therefore, it is necessary to predict the physical and thermodynamic properties of compounds comprising the reactive system using a group contribution method. In this case, we used the method of Joback and Reid.<sup>19</sup> For this study, we use the Aspen Plus simulator, which is widely employed in the design process on an industrial scale. It is convenient to remark that the simulator database of Aspen Plus does not include some compounds to be used during the course of this work, for example, 4-MDBT and 4,6-DMDBT, and some reaction products of hydrodesulfurization (e.g., 3-MCHT). Therefore, it is vitally important the definition of these components in the simulator and performing the calculation of their properties. These properties have been calculated using the method of Joback and Reid.<sup>19</sup> On the other hand, we have employed the Peng–Robinson EoS as thermodynamic model to calculate the vapor–liquid equilibrium. The feed mixture used as case of study in this work is that used in the paper of Viveros-García et al.<sup>4</sup> This mixture contains the most representative compounds of sulfur and a mixture of five compounds present in the diesel paraffinic, which is given in Table 1.

## 3. DESCRIPTION OF THE MULTIOBJECTIVE OPTIMIZATION METHOD USED FOR PROCESS ANALYSIS

To the best of the author's knowledge, there are not studies in the literature on the rigorous multiobjective optimization of the

**Table 2.** Optimization Variables and Bounds Used in the Multiobjective Optimization of the Process Schemes for the HDS Process

design variable	type of variable		scheme					
	continuous	discrete	DRSI	DRSII	DRI	DRSL	DR3R	RD
temperature in $F_1$ ( $^{\circ}\text{C}$ )	×		[170 190]	[170 190]	[170 190]	[170 190]	[170 190]	[170 190]
number of stages in column C, $N_C$		×	[7 30]	[5 30]	[3 29]	[5 30]	[4 29]	[5 30]
feed stage in column C, $N_F$		×	[4 29]	[3 29]	[2 29]	[2 29]	[2 29]	[2 29]
pressure in column C (atm)	×		[1 10]	[1 10]	[1 10]	[1 10]	[1 10]	[1 30]
distillate flow rate in C (lb mol/h)	×		[550 650]	[30 45]	[30 45]	[30 45]	[30 45]	[300 380]
reflux ratio in column C	×		[1 10]	[0.1 10]	[0.1 10]	[0.1 10]	[0.1 10]	[0.1 10]
temperature in exchanger $\text{HEX}_1$ ( $^{\circ}\text{C}$ )	×		[250 350]	[250 350]	[250 350]	[250 350]	[250 350]	
pressure in exchanger $\text{HEX}_1$ (atm)	×		[25 35]	[25 35]	[25 35]	[25 35]	[25 35]	
temperature in exchanger $\text{HEX}_2$ ( $^{\circ}\text{C}$ )	×		[250 400]	[250 400]	[250 400]	[250 400]	[250 400]	
pressure in exchanger $\text{HEX}_2$ (atm)	×		[25 35]	[25 35]	[25 35]	[25 35]	[25 35]	
temperature in exchanger $\text{HEX}_3$ ( $^{\circ}\text{C}$ )	×						[250 400]	
pressure in exchanger $\text{HEX}_3$ (atm)	×						[25 35]	
feed stage, $F_2$ , $N_{F2}$		×						[2 29]
hydrogen flow rate in $F_2$ (lb mol/h)	×		[250 350]	[250 350]	[250 350]	[250 350]	[250 350]	[250 350]
hydrogen flow rate in $F_3$ (lbmol/h)	×		[250 350]	[250 350]	[250 350]	[250 350]	[250 350]	
hydrogen flow rate in $F_4$ (lb mol/h)	×						[250 350]	
amount of catalyst in the reactor $R_1$ (kg)	×		[5 20]	[5 20]	[5 20]	[5 20]	[5 20]	
amount of catalyst in the reactor $R_2$ (kg)	×		[1000 3000]	[1000 3000]	[1000 3000]	[1000 3000]	[1000 3000]	
amount of catalyst in the reactor $R_3$ (kg)	×						[1000 3000]	
stages of reactive zone I, $N_{II}$ , $N_{II}$		×						[2 27]
stages of reactive zone II, $N_{III}$ , $N_{III}$		×						[4 29]
stage of side flow rate $S_1$ in column C, $N_{S1}$		×	[2 29]	[2 29]			[3 29]	
side flow rate $S_1$ in column C (lb mol/h)	×		[0.1 50]	[0.1 50]			[0.1 50]	
stage of side flow rate $S_2$ in column C, $N_{S2}$		×	[2 29]	[2 29]		[2 29]		
side flow rate $S_2$ in column C (lb mol/h)	×		[0.1 50]	[0.1 50]		[0.1 50]		
feed stage of flow rate $E_1$ in column C, $N_{E1}$		×	[2 29]					
feed stage of flow rate $E_1$ in column C, $N_{E2}$		×	[2 29]					
amount of catalyst in reactive zone I (kg)	×							[100 1000]
amount of catalyst in reactive zone II (kg)	×							[100 1000]

HDS process. In this study, we have used a multiobjective optimization method based on differential evolution with taboo list (MODE-TL), which has been developed by Sharma and Rangaiah.<sup>20,21</sup> Specifically, this MODE-TL algorithm includes classical differential evolution steps, adaptation for multiple objectives (selection of individuals for subsequent generations), taboo list and taboo check, and a convergence criterion based on the number of generations.<sup>20,21</sup> According to Sharma and Rangaiah,<sup>20,21</sup> a population of NP individuals with D-dimension, given by the number of decision variables, is initialized randomly inside the bounds of decision variables. A mutant vector is generated by adding the scaled difference of two randomly selected individuals with another randomly chosen individual. Elements of this mutant vector compete with those of target vector, with probability Cr, to generate a trial vector. The Taboo list concept of Taboo Search is used in the multiobjective optimization algorithm to avoid the revisit of search space by keeping a record of recently visited points. Taboo list is randomly initialized using the initial population and continuously updated with the newly generated trial individuals. This taboo check is implemented in the generation step of trial vector, and the new trial individual is generated repeatedly until it is not near to any individual in the taboo list. Objective functions and constraints are evaluated for this new trial individual. Total NP trial individuals are generated by the repetition of above steps. The newly generated NP trial vectors are combined with the parent population to form a combined population with total 2NP individuals. This combined

population undergoes nondominated sorting and ranking accordingly. Individuals with the same nondominated rank are further ranked on the basis of crowding distance. The best NP individuals are used as the population in the subsequent generation.<sup>20,21</sup> More details of this algorithm are provided by Sharma and Rangaiah.<sup>20,21</sup> Note that this multiobjective optimization method has been successfully used, for example, in the design of biodiesel production process.<sup>21</sup>

Herein, it is convenient to remark that, in a study conducted by Bisowarno et al.<sup>22</sup> for the production of ethyl *tert*-butyl ether, a side reactor was added to a distillation column to remove some design problems. These lateral reactors have the advantage of reducing the charge of catalyst in the column, which results in a decrease in size of the reaction section and leads to a reduction in the cost of the column. From the point of view of process control, the conversion of reactants can be controlled at the outlet of the reactor and the purity of the product is controlled in the distillation column, further conditions including side reactor operations are not limited by distillation. Based on this concept, Plaza-Rosas<sup>15</sup> carried out the conceptual synthesis of DRS systems for HDS process. However, this author has not performed the design and formal optimization of synthesized systems (Figure 1a–e). Taking as a starting point the conceptual design of the distillation column reactive (DR) proposed by Viveros-García et al.,<sup>4</sup> the analysis of gas oil studied by Ma et al.,<sup>23</sup> and the work on the concept of a lateral reactor by Baur and Krishna,<sup>24</sup> the concept of a lateral distillation reactor is proposed in the HDS of diesel as an

alternative to a conventional HDS process. This design process is used to separate the diesel into two fractions, as suggested by Ma et al.,<sup>23</sup> a light fraction to treat sulfur compounds with low point boiling. In this case and, considering the mixture models to be used, we refer to thiophene and benzothiophene, and a heavy fraction is comprised of DBT and 4,6-DMDBT. This idea has been handled by Viveros-García<sup>4</sup> since the purpose of placing two reagent zones, each with a different catalyst in the reaction column, is to carry out the HDS of light sulfur compounds in the rectifier zone with CoMo catalyst and the HDS of heavy sulfur compounds using NiMo catalyst in the stripper zone. Then, in the case of distillation with side reactors, each of these reactive areas found inside the distillation column (Figure 1f) would be replaced by a hydrodesulfurization reactor outside, as shown in Figure 1a–e, where the first reactive zone (of the reactive distillation, see Figure 1f) containing the CoMo catalyst is replaced by an external reactor. The feed is taken from a side stream from the distillation column, and also, it uses a CoMo catalyst. The hydrogen feed will not be into the column; it will be directly fed to the reactor.

Similarly, the second reactive zone II (Figure 6f) is replaced by another HDS reactor that is operated with NiMo catalyst. The effluent from both reactors may or may not be recycled to the distillation column, depending on the conversion of products that has been reached in the reactors.

In order to optimize the DRS schemes (using as lateral reactor a plug flow model as proposed in Aspen simulator) involved in the HDS process, we used this MODE-TL algorithm (which is programmed in excel software) coupled to an Aspen ONE Aspen Plus simulator. The connection of Excel with Aspen Plus includes the flow of data between these programs. The vector values of decision variables ( $V_x$ ) are sent from Microsoft Excel using DDE (dynamic data exchange) by COM technology. These values are attributed in Excel to the corresponding process variables ( $V_x$ ) and then sent to Aspen Plus. Note that using the COM technology, it is possible to add code such that the applications behave as an Object Linking and Embedding (OLE) automation server. After running the rigorous simulation, Aspen Plus returns to MS Excel the vector of results ( $V_r$ ). Note that the CPU time for each optimization step is determined mainly by the convergence time required by the Aspen Plus simulator, which ensures rigorous process simulation results. The optimization was carried out on a Dell computer with Intel Core i7CPU 930 processor at 2.80 GHz, 6.00 GB of RAM, and Windows 7 Ultimate. Specifically, for process design of these separation schemes, we have performed a multiobjective optimization where TAC, CO<sub>2</sub> emissions (which is also an indicator of energy consumption in the system), and the amount of sulfur compounds are the simultaneous optimization targets. This design problem is challenging due to the presence of both continuous and discontinuous decision variables subject to several constraints. Details of this MOO problem for each process configuration are given in Table 2. As can be seen from Table 2, the selected variables are the most relevant to the design of a distillation column and heat exchangers.<sup>4,13</sup> In the present study, TAC is estimated as the sum of the annual operation cost and the annualized investment cost for the process. The investment costs of equipment are estimated by the cost equations shown in the work of Turton et al.<sup>25</sup> that are updated with the CEPCI (Chemical Engineering Process Cost Index), while CO<sub>2</sub> emissions are calculated by the technique proposed by Gadalla et al.<sup>26</sup> For the DRS options and RD used in the HDS process,

the multiobjective optimization problem can be stated as follows:

$$\min(\text{TAC}, \text{CO}_2 \text{ emissions}, \text{amount of sulfur compounds}) \quad (1)$$

subject to inequality constraints reported in Table 3 for each DRS scheme and RD configuration. Note that these constraints

**Table 3. Constraints of the Problem for the Multiobjective Optimization of HDS Process**

constraints	DRSI	DRSII	DRI	DRSL	DR3R	RD
$N_C > N_F$				×		
$N_C > N_F > N_{S2}$					×	×
$N_C \neq N_F \neq N_{S2}$				×		×
$N_C > N_F > N_{S2} > N_{S1}$	×	×				
$N_C \neq N_F \neq N_{S2} \neq N_{S1}$	×	×				
$N_C > N_{E1} > N_{E2}$	×					
$N_C \neq N_{E1} \neq N_{E2}$	×					
$N_C > N_F > N_{F2}$						×
$N_C > N_{II} > N_{III} > N_{II} > N_{II}$						×

imply physical restrictions for the design variables and/or operating conditions of proposed schemes. A penalty function approach has been used for handling these constraints.

#### 4. RESULTS AND DISCUSSION

This section shows the results obtained for the different case studies analyzed. In carrying out the optimization with the

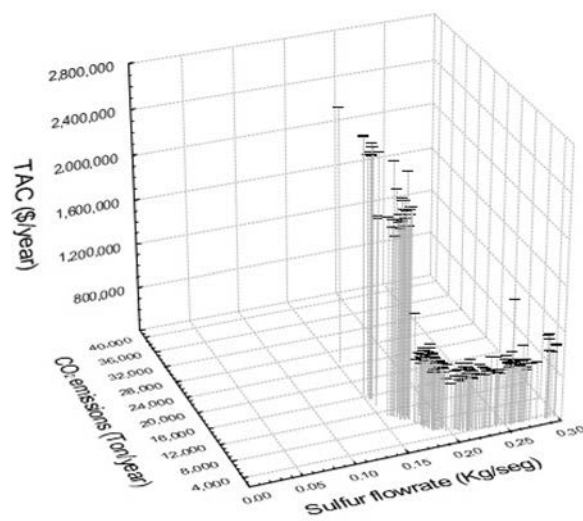


**Figure 3.** Pareto front for DRSI.

MODE-TL method, we have used the following algorithm parameters: a population of 200 individuals, Cr = 0.3, taboo radius = 0.02, mutation rate = 0.5, and a maximum number of generations = 750. This parameter tuning of MODE-TL was performed based on preliminary trial calculations. With these conditions, MODE-TL showed a good convergence performance and it generated the respective Pareto fronts for the DRS and RD schemes in the HDS process.

With this information (i.e., Pareto fronts), it is possible to identify the operating conditions of the separation systems to minimize the TAC, CO<sub>2</sub> emissions and sulfur flow rate. Below it is presented the analysis for some of the optimization

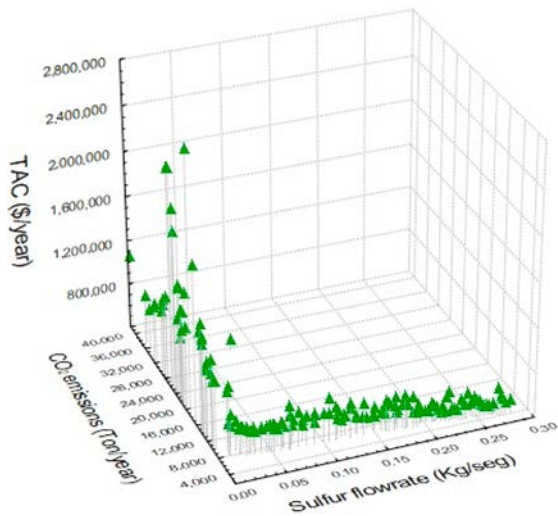


Figure 4. Pareto front for DRSII.

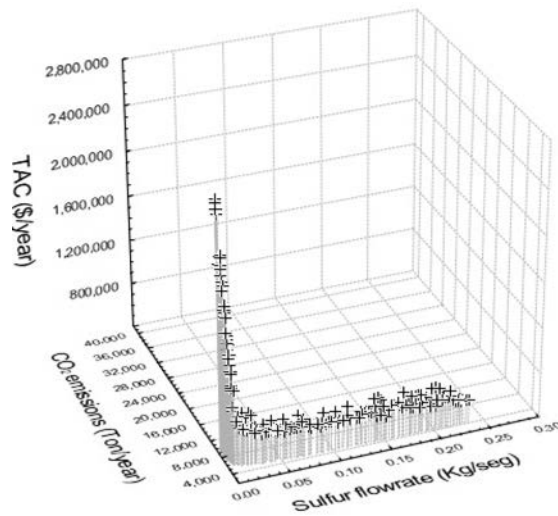


Figure 7. Pareto front for DR3R.

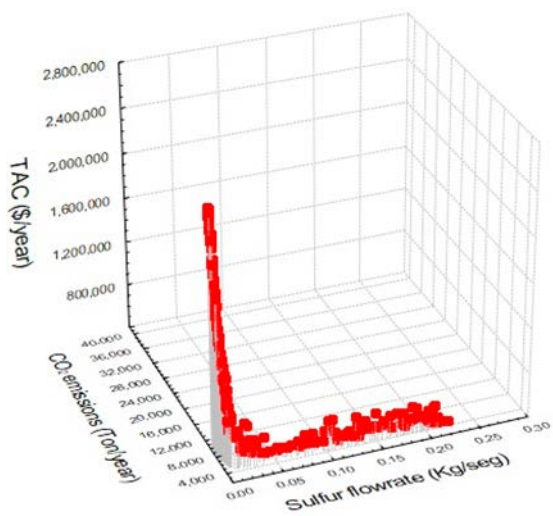


Figure 5. Pareto front for DRI.

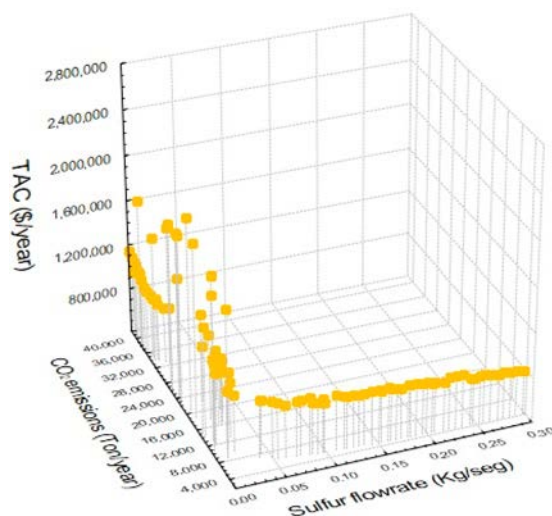


Figure 8. Pareto front for RD.

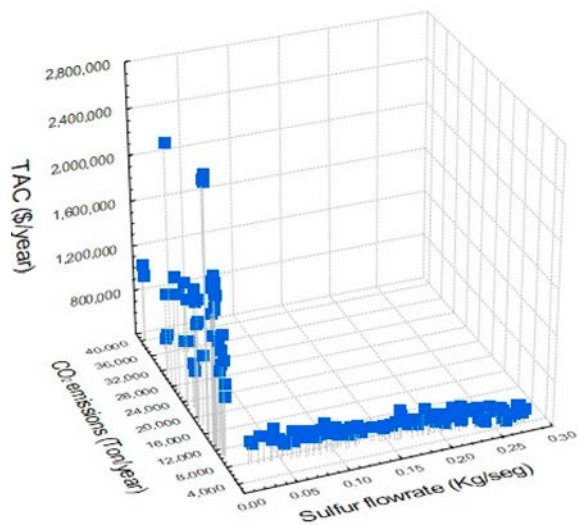


Figure 6. Pareto front for DRSL.

variables considered in the multiobjective optimization of all schemes.

With illustrative purposes, we studied the effect of the temperature of the feed mixture on the TAC for all design schemes. For Scheme DRSI, the value of TAC is the highest of all schemes with a value greater than  $3.80 \times 10^6$  USD/y. Behavior in Scheme DRSI is due to the presence of recirculation, since the column operates with a large amount of flow rate, affecting the value of reboiler duty, column diameter, and finally, these conditions are reflected in the TAC. Also, we have conducted an analysis of the effect of feed stage on the TAC. Overall, Scheme DRSI presented the highest costs, while the lowest costs are obtained for Scheme DRSL.

In general, it can be observed for all schemes, the trend is, while the flow decreases sulfur diesel fuel, TAC increases, i.e., the cost to be paid for doing the HDS process increases when the diesel requires less amount of sulfur at the end of the process, as can be seen in the analysis presented below.

For Scheme DRSI, the Pareto front obtained with the algorithm MODE-TL is reported in Figure 3. The solution with the lowest TAC is 809,433 USD/y, and it presents 9089.31 tons/y of CO<sub>2</sub> emissions and 0.20219 kg/s of sulfur flow at the end of the HDS process. The cleanest solution for this scheme has 3099.22 tons/y of CO<sub>2</sub> emissions, but diesel at the end of

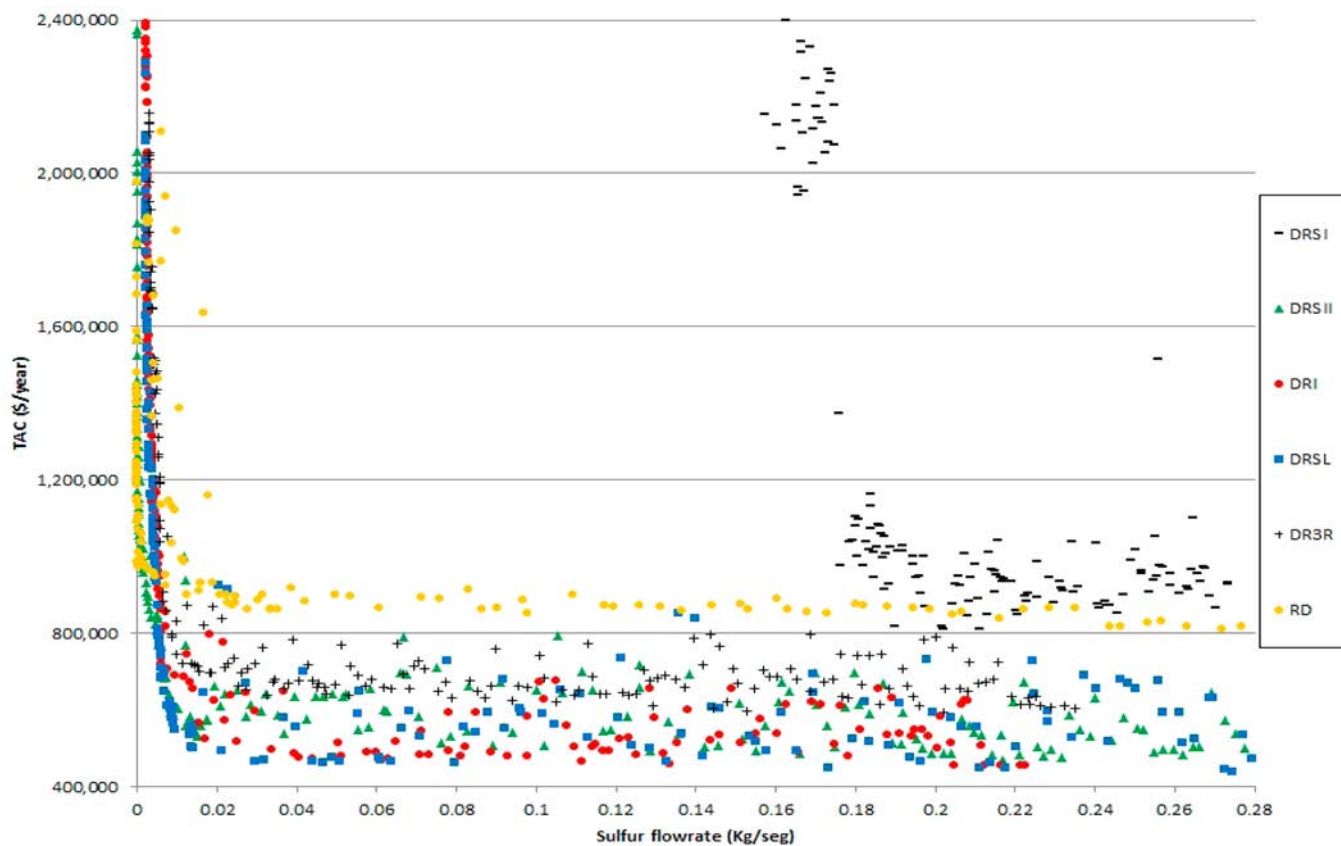


Figure 9. Comparison of Pareto fronts for the HDS process using all separation system schemes. TAC vs sulfur flow rate.

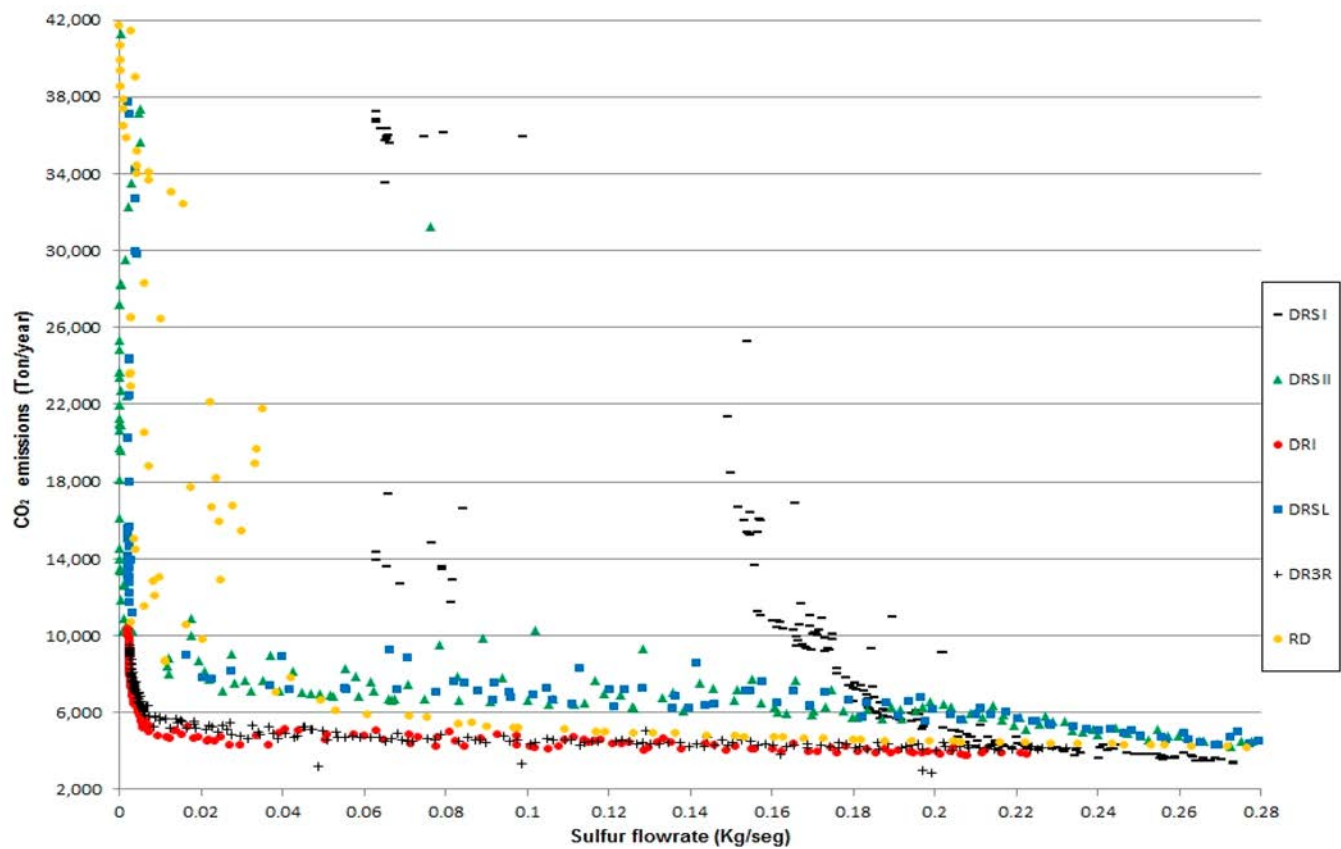


Figure 10. Comparison of Pareto fronts for HDS process using all separation system schemes. CO<sub>2</sub> emissions vs sulfur flow rate.

**Table 4. Designs with Minimum TAC Obtained from Pareto Solutions for All Separation System Schemes Analyzed in the HDS Process**

	DRSI	DRSII	DRI	DRSL	DR3R	RD
temperature in $F_1$ ( $^{\circ}\text{C}$ )	184.73	188.14	189.75	189.36	189.94	189.73
number of stages in column C	27	27	5	11	12	29
feed stage in column C	25	6	4	3	3	6
pressure in column C (atm)	3.43	1.01	1.00	1.01	1.01	3.40
distillate flow rate in C (lb mol/h)	610.33	31.84	30.09	30.09	30.01	325.95
reflux ratio in column C	1.01	0.16	0.11	0.11	0.10	0.10
temperature in exchanger $\text{HEX}_1$ ( $^{\circ}\text{C}$ )	284.69	301.03	258.52	252.55	257.17	
pressure in exchanger $\text{HEX}_1$ (atm)	27.46	33.64	29.67	29.18	33.81	
temperature in exchanger $\text{HEX}_2$ ( $^{\circ}\text{C}$ )	365.25	300.93	300.52	264.15	317.01	
pressure in exchanger $\text{HEX}_2$ (atm)	27.90	32.12	30.62	28.59	25.32	
temperature in exchanger $\text{HEX}_3$ ( $^{\circ}\text{C}$ )					300.80	
pressure in exchanger $\text{HEX}_3$ (atm)					27.76	
feed stage, $F_2$						28
hydrogen flow rate in $F_2$ (lb mol/h)	317.62	255.79	251.12	253.31	282.20	250.42
hydrogen flow rate in $F_3$ (lb mol/h)	280.83	332.36	255.28	259.98	261.97	
hydrogen flow rate in $F_4$ (lb mol/h)					251.86	
amount of catalyst in the reactor $R_1$ (kg)	8.99	15.26	6.52	12.90	11.87	
amount of catalyst in the reactor $R_2$ (kg)	1314.64	1942.70	1052.50	1082.21	1062.14	
amount of catalyst in the reactor $R_3$ (kg)					1642.00	
stages of reactive zone I						3–4
stages of reactive zone II						7–28
stage of side flow rate $S_1$ in column C	26	8			4	
side flow rate $S_1$ in column C (lb mol/h)	48.76	40.80			47.95	
stage of side flow rate $S_2$ in column C	15	3		4		
side flow rate $S_2$ in column C (lb mol/h)	39.29	0.59		48.36		
diameter of column C (mts)	1.18	0.61	0.48	0.59	0.59	1.37
feed stage of flow rate $E_1$ in column C, $N_{E1}$	26					
feed stage of flow rate $E_1$ in column C, $N_{E2}$	5					
amount of catalyst in reactive zone I (kg)						718.16
amount of catalyst in reactive zone II (kg)						988.85
temperature of partial condenser ( $^{\circ}\text{C}$ )						200.12
TAC (USD/y)	809,433.10	471,003.25	455,124.37	441,719.86	594,512.36	803,561.77
$\text{CO}_2$ emissions (ton/y)	9,089.31	5,888.86	3,863.31	4,597.29	4,464.52	6094.26
sulfur flow rate (ppm)	0.2022	0.21671	0.22128	0.26081	0.20214	0.05326

the process comes with a flow of 0.29682 kg/s of sulfur in the processed mixture. The solution with the lowest sulfur flow of 0.060 08 kg/s shows 53 135.52 tons/y of  $\text{CO}_2$ , and it has a TAC of 3,668,683.55 USD/y. Clearly, we can see that these design objectives are in competition.

Figure 4 shows the set of Pareto solutions for Scheme DRSII where we can observe a very different behavior to Scheme DRSI. This behavior is due in part to the currents of distillate and bottom are connected with side streams, which imposes certain restrictions on the process. The most economical process for this scheme shows a TAC of 471,003.25 USD/y and 5888.86 tons/y of  $\text{CO}_2$  emissions, and this process is producing diesel with sulfur flow of 0.21 671 kg/s. The point that has the least amount of  $\text{CO}_2$  emissions with 4184.47 tons/y generates a TAC of 523,941.33 USD/y and a sulfur flow 0.282 83 kg/s.

Figure 5 shows the relationship between the TAC,  $\text{CO}_2$  emissions, and the flow of sulfur in diesel for the Scheme DRI. The trend is that as sulfur flow is reduced in the output flow rates, the TAC is considerably increased. Also,  $\text{CO}_2$  emissions are increasing slowly to a point, about 0.005 kg/s, where this increment is remarkable.

The Pareto front for Scheme DRSL, see Figure 6, shows the different feasible solutions provided by the multiobjective

algorithm. We can see that while reducing the sulfur flow in both streams of distillate and in the bottom,  $\text{CO}_2$  emissions will increase gradually to an outflow 0.022 86 kg/s of sulfur in the products at the end of the process. From this solution,  $\text{CO}_2$  emissions increase considerably. The solutions of the Pareto front show a very similar trend to the Scheme DRSII, and this is because both schemes have at least one side stream.

Figure 7 shows the diversity of optimal solutions in the Pareto front for Scheme DR3R, which correspond to different design parameters. Scheme DR3R shows a trend very similar to Scheme DRI. Also, both schemes show a uniform distribution of Pareto solutions. On the other hand, Figure 8 presents the TAC as a function of  $\text{CO}_2$  and sulfur flow rate in output currents of RD column. As can be seen, this design has higher operating costs than those reported for DRS systems.

Figure 9 shows that Scheme DRSI implies the highest TAC of all schemes. This is because Scheme DRSI requires the greatest number of stages and distillate flow, increasing the reboiler duty required to perform the separation. For Scheme DRSI, see Figures 9 and 10, the flow of the sulfur compounds is very high, and this is because the amount sent to the reactor is small. Also, the amount of both compounds to be extracted from the distillate and bottom streams, respectively, is minimum. On the other hand, for example, in Figure 9, the

**Table 5. Designs with Minimum CO<sub>2</sub> Emissions Obtained from Pareto Solutions for All Separation System Schemes Analyzed in HDS Process**

	DRSI	DRSII	DRI	DRSL	DR3R	RD
temperature in F <sub>1</sub> (°C)	189.28	188.12	189.98	188.58	189.97	189.66
number of stages in column C	29	18	27	26	23	29
feed stage in column C	27	10	6	14	4	5
pressure in column C (atm)	1.16	1.06	1.00	1.00	1.00	2.20
distillate flow rate in C (lb mol/h)	591.94	38.34	30.30	37.73	30.43	325.18
reflux ratio in column C	1.04	0.82	0.12	0.54	0.10	0.10
temperature in exchanger HEX <sub>1</sub> (°C)	252.10	294.35	253.42	330.06	250.26	
pressure in exchanger HEX <sub>1</sub> (atm)	26.33	34.23	34.15	28.46	32.41	
temperature in exchanger HEX <sub>2</sub> (°C)	277.97	372.98	300.40	333.06	300.43	
pressure in exchanger HEX <sub>2</sub> (atm)	32.14	27.90	33.42	27.74	33.77	
temperature in exchanger HEX <sub>3</sub> (°C)					304.93	
pressure in exchanger HEX <sub>3</sub> (atm)					28.86	
feed stage, F <sub>2</sub>						28
hydrogen flow rate in F <sub>2</sub> (lb mol/h)	304.10	271.00	252.87	270.37	252.79	250.28
hydrogen flow rate in F <sub>3</sub> (lb mol/h)	286.48	261.25	250.35	322.36	270.54	
hydrogen flow rate in F <sub>4</sub> (lb mol/h)					252.12	
amount of catalyst in the reactor R <sub>1</sub> (kg)	12.57	11.18	15.23	13.81	17.02	
amount of catalyst in the reactor R <sub>2</sub> (kg)	1513.33	1873.84	1896.75	2318.48	2443.72	
amount of catalyst in the reactor R <sub>3</sub> (kg)					433.72	
stages of reactive zone I						3–4
stages of reactive zone II						7–28
stage of side flow rate S <sub>1</sub> in column C	28	3			5	
side flow rate S <sub>1</sub> in column C (lb mol/h)	4.01	48.39			24.04	
stage of side flow rate S <sub>2</sub> in column C	17	6		17		
side flow rate S <sub>2</sub> in column C (lb mol/h)	0.90	43.89		25.37		
diameter of column C (mts)	1.22	0.75	0.62	0.70	0.59	1.32
feed stage of flow rate E <sub>1</sub> in column C, N <sub>E1</sub>	28					
feed stage of flow rate E <sub>1</sub> in column C, N <sub>E2</sub>	5					
amount of catalyst in reactive zone I (kg)						340.90
amount of catalyst in reactive zone II (kg)						998.23
temperature of partial condenser (°C)						182.02
TAC (USD/y)	1,062,918.98	523,941.33	623,389.91	523,111.75	791,949.30	897,627.80
CO <sub>2</sub> emissions (ton/y)	3,099.22	4,184.47	3,770.68	4,219.05	3,996.23	4,057.22
sulfur flow rate (ppm)	0.29682	0.28283	0.20747	0.27881	0.20019	0.29748

solution of Scheme DRSI with a flow of sulfur from 0.2968 kg/s and TAC of 1,062,919 USD/y is not an adequate solution compared to other schemes, based on the operating cost. This same solution with 0.2968 kg/s of sulfur flow, in Figure 10, presents the best value of CO<sub>2</sub> emissions of Scheme DRSI and even of all schemes. Therefore, for Scheme DRSI, the recirculation in the distillation column increases the TAC, reduces the conversion of reagents, but also greater flow of sulfur compounds at the end of the process generates a clean process (see Figure 10). It is important to note that the reduction of sulfur flow is the most important objective in the design of this process. In general, the reduction of sulfur in diesel increases the operating cost (Figure 9) and CO<sub>2</sub> emissions (Figure 10). The search for a balance between TAC and CO<sub>2</sub> emissions requires careful consideration for the design of HDS process.

The DR process presents designs with sulfur flow in small quantities for the output currents. However, DR has more CO<sub>2</sub> emissions, and this design is usually more expensive if the sulfur flow is very low, below 0.001 kg/s; see Figures 9 and 10.

Schemes DRI and DRSL show the best values of TAC, if the sulfur flow is reduced to 0.008 kg/s, while Schemes III and V are the solutions with the smallest amount of CO<sub>2</sub> emissions for the same flow. Therefore, a good choice for the HDS

process is the Scheme DRI, as it is a clean process and has a low cost compared to other schemes and DR columns (see Figures 9 and 10). For illustrative purposes, Tables 4–6 show some selected solutions obtained from the Pareto fronts of the various schemes discussed in the HDS process. Again, we confirm that Scheme DRI offers the best operating conditions for the HDS process.

## 5. CONCLUSIONS

In this study, we report the multiobjective optimization for the design of five DRS schemes in the HDS process. It is important to recall that the Pareto front of these schemes includes three design objectives: TAC, CO<sub>2</sub> emissions, and amount of sulfur compounds. It is important to remark that the reduction of sulfur compounds is the most important objective in the design of this process. In general, the reduction of the amount of sulfur compounds increases the TAC and CO<sub>2</sub> emissions. However, we can identify proper operating conditions where TAC can be significantly reduced. Therefore, these trades-offs of TAC and CO<sub>2</sub> emissions call for careful consideration for the design of this process in diesel production. Overall, results show that the separation schemes of distillation with side reactors may offer a better performance for HDS process in comparison to reactive distillation. In particular, the scheme DRI offers the best trade-

**Table 6. Designs with Minimum Sulfur Flow Rate Obtained from Pareto Solutions for All Separation System Schemes Analyzed in HDS Processes**

	DRSI	DRSII	DRI	DRSL	DR3R	RD
temperature in F <sub>1</sub> (°C)	184.65	189.46	180.18	188.57	186.24	189.51
number of stages in column C	27	28	29	29	29	29
feed stage in column C	25	10	27	19	26	18
pressure in column C (atm)	3.81	1.04	1.00	1.01	1.00	14.69
distillate flow rate in C (lb mol/h)	643.61	39.18	45.00	44.96	44.95	325.30
reflux ratio in column C	1.05	2.88	7.67	8.74	6.11	0.32
temperature in exchanger HEX <sub>1</sub> (°C)	279.06	332.17	339.09	311.55	316.90	
pressure in exchanger HEX <sub>1</sub> (atm)	27.10	32.91	25.42	29.66	33.49	
temperature in exchanger HEX <sub>2</sub> (°C)	331.99	373.58	385.59	349.33	397.12	
pressure in exchanger HEX <sub>2</sub> (atm)	25.73	30.22	30.09	33.39	29.86	
temperature in exchanger HEX <sub>3</sub> (°C)					308.87	
pressure in exchanger HEX <sub>3</sub> (atm)					28.31	
feed stage, F <sub>2</sub>						23
hydrogen flow rate in F <sub>2</sub> (lb mol/h)	270.00	304.43	260.96	278.84	281.19	281.23
hydrogen flow rate in F <sub>3</sub> (lb mol/h)	293.59	293.25	323.36	288.67	291.55	
hydrogen flow rate in F <sub>4</sub> (lb mol/h)					257.06	
amount of catalyst in the reactor R <sub>1</sub> (kg)	9.91	11.80	18.80	15.09	15.47	
amount of catalyst in the reactor R <sub>2</sub> (kg)	2298.38	2617.83	1465.44	2658.79	1503.92	
amount of catalyst in the reactor R <sub>3</sub> (kg)					433.72	
stages of reactive zone I						6–7
stages of reactive zone II						19–23
stage of side flow rate S <sub>1</sub> in column C	26	22			27	
side flow rate S <sub>1</sub> in column C (lb mol/h)	47.81	1.41			0.11	
stage of side flow rate S <sub>2</sub> in column C	9	4		20		
side flow rate S <sub>2</sub> in column C (lb mol/h)	8.69	36.53		24.08		
diameter of column C (mts)	1.71	1.02	1.59	1.70	1.43	2.05
feed stage of flow rate E <sub>1</sub> in column C, N <sub>E1</sub>	26					
feed stage of flow rate E <sub>1</sub> in column C, N <sub>E2</sub>	5					
amount of catalyst in reactive zone I (kg)						808.83
amount of catalyst in reactive zone II (kg)						987.09
temperature of partial condenser (°C)						151.77
TAC (USD/y)	3,668,683.55	1,216,199.92	2,497,643.58	2,647,767.03	2,536,990.38	1,978,496.51
CO <sub>2</sub> emissions (ton/y)	53,135.52	79,796.96	10,114.67	15,281.84	9,537.54	6,7985.53
sulfur flow rate (ppm)	0.06008	6.034 × 10 <sup>-05</sup>	0.00234	0.00217	0.00257	0.00015

offs for TAC, sulfur flow rate, and CO<sub>2</sub> emissions for the HDS process.

## APPENDIX A

The costing of a distillation column (carbon steel construction) was estimated by the cost equations shown in the work of Turton et al.<sup>25</sup> that are updated with the CEPCI (Chemical Engineering Process Cost Index). For comparison, a single value of CEPCI is selected as a starting value for the year that this research was conducted. The total column cost is the sum of the installed cost of column shell and the installed cost of column trays. On the other hand, the sizing and costing of heat exchangers were calculated. The cost of heat exchangers can be correlated as a function of the surface area assuming shell and tube, floating head, and carbon steel construction. The installation prices are updated by the CEPCI index. The capital cost (purchase plus installation cost) is annualized over a period which is often referred to as plant lifetime:

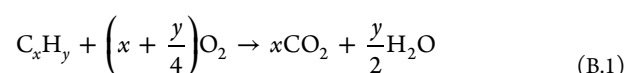
$$\text{annual capital cost} = \text{capital cost} / \text{plant lifetime} \quad (\text{A.1})$$

$$\begin{aligned} \text{total annual cost (TAC)} \\ = \text{annual operating cost} + \text{annual capital cost} \end{aligned} \quad (\text{A.2})$$

Operating costs were assumed to be just utility cost (steam and cooling water). Plant life = 10 y. Operating hours = 8400 h/y.

## APPENDIX B

Fuel combusts when mixed with air, producing CO<sub>2</sub> according to the following stoichiometric equation:



where  $x$  and  $y$  denote the number of carbon, C, and hydrogen, H, atoms, respectively, present in the fuel compositions and where complete oxidation of carbon is assumed.

In the combustion of fuels, air is assumed to be in excess to ensure complete combustion, so that no carbon monoxide is formed. CO<sub>2</sub> emissions, [CO<sub>2</sub>]<sub>Emiss</sub> (kg/s), are related to the amount of fuel burnt, Q<sub>Fuel</sub> (kW), in a heating device as follows:

$$[\text{CO}_2]_{\text{Emiss}} = \left(\frac{Q_{\text{Fuel}}}{\text{NHV}}\right) \left(\frac{C\%}{100}\right) \alpha \quad (\text{B.2})$$

where  $\alpha$  (= 3.67) is the ratio of molar masses of CO<sub>2</sub> and C, while NHV (kJ/kg) represents the net heating value of a fuel with a carbon content of C%. Equation B.2 shows that both the

fuel used and the heating device affect the amount of CO<sub>2</sub> produced.

Boilers produce steam from the combustion of fuel. This steam is delivered to the process at the temperature required by the process or obtained at a higher temperature and then throttled. In distillation systems, steam is used either for heating purposes, indirectly in reboilers, or as a direct stripping agent in so-called steam-distillations, such as crude oil units. The flame temperature is lower in a boiler than in a furnace because the heat of combustion is removed immediately from the steam. However, the same theoretical flame temperature of 1800 °C may still be used. The stack temperature of 160 °C is also used in the calculations. The amount of fuel burnt can be as follows:

$$Q_{\text{Fuel}} = \frac{Q_{\text{Proc}}}{\lambda_{\text{Proc}}} (h_{\text{Proc}} - 419) \frac{T_{\text{FTB}} - T_0}{T_{\text{FTB}} - T_{\text{Stack}}} \quad (\text{B.3})$$

where  $\lambda_{\text{Proc}}$  (kJ/kg) and  $h_{\text{Proc}}$  (kJ/kg) are the latent heat and enthalpy of steam delivered to the process, respectively, while  $T_{\text{FTB}}$  (°C) is the flame temperature of the boiler flue gases. The above equation is obtained from a simple steam balance around the boiler to relate the amount of fuel necessary in the boiler to provide a heat duty of  $Q_{\text{proc}}$ ; and the boiler feedwater is assumed to be at 100 °C with an enthalpy of 419 kJ/kg. Equations B.2 and B.3 can be used to calculate the CO<sub>2</sub> emissions from steam boilers.

## AUTHOR INFORMATION

### Corresponding Author

\*Tel.: +52(473)7320006. E-mail: gsegovia@ugto.mx.

### Notes

The authors declare no competing financial interest.

## ACKNOWLEDGMENTS

This research project was supported by Universidad de Guanajuato and Instituto Tecnológico de Aguascalientes (México).

## REFERENCES

- (1) Froment, G. F.; Depauw, G. A.; Vanrysselberghe, V. Kinetic Modeling and Reactor Simulation in Hydrodesulfurization of Oil Fractions. *Ind. Eng. Chem. Res.* **1994**, *33*, 2975.
- (2) Al-Daous, M. A.; Ali, S. A. Deep Desulfurization of Gas Oil over NiMo Catalysts Supported on Alumina–Zirconia Composites. *Fuel* **2012**, *97*, 662.
- (3) Rodríguez, M. A.; Elizalde, I.; Ancheyta, J. Comparison of Kinetic and Reactor Models to Simulate a Trickle-Bed Bench-Scale Reactor for Hydrodesulfurization of VGO. *Fuel* **2012**, *100*, 91.
- (4) Viveros-García, T.; Ochoa-Tapia, J. A.; Lobo-Oehmichen, R.; de los Reyes-Heredia, J. A.; Pérez-Cisneros, E. S. Conceptual Design of a Reactive Distillation Process for Ultra-Low Sulfur Diesel Production. *Chemical Engineering Journal* **2005**, *106*, 119.
- (5) Singhal, G. H.; Espino, R. L.; Sobel, J. E.; Huff, G. A., Jr. Hydrodesulfurization of Sulfur heterocyclic Compounds Kinetics of Dibenzothiophene. *J. Catal.* **1981**, *67*, 457.
- (6) Ho, T. C.; Sobel, J. E. Kinetics of Dibenzothiophene Hydrodesulfurization. *J. Catal.* **1991**, *128*, 581.
- (7) Houalla, M.; Broderick, D. H.; Sapre, A. V.; Nag, N. K.; DeBeer, V.H. J.; Gates, B. C.; Kwart, H. Hydrodesulfurization of Methylsubstituted Dibenzothiophenes Catalyzed by Sulfided Co-Mo/ $\gamma$ -Al<sub>2</sub>O<sub>3</sub>. *J. Catal.* **1980**, *61*, 523.
- (8) Sakanishi, K.; Ma, X.; Mochida, I. Three-stage Deep Hydrodesulfurization of Diesel Fuel under 30 kg/cm<sup>2</sup> H<sub>2</sub> Pressure without Color Development. *J. Jpn. Pet. Znst.* **1993**, *36*, 145.

(9) Ma, X.; Sakanishi, K.; Mochida, I. Hydrodesulfurization Reactivities of Various Compounds in Diesel Fuel. *Ind. Eng. Chem. Res.* **1994**, *33*, 218.

(10) Knudsen, K. G.; Cooper, B. H.; Topsoe, H. Catalyst and Process Technologies for Ultra Low Sulfur Diesel. *Appl. Catal. Gen.* **1999**, *189*, 205.

(11) Topsoe, H.; Massoth, F. E.; Clausen, B. S. Hydrotreating catalyst. *Catalyst Science and Technology*; Anderson, J. R., Boudart, M., Eds.; Springer Verlag: Berlin, 1996; Vol. 11.

(12) Van Hasselt, B. W.; Lebens, P. J. M.; Calis, H. P. A.; Kapteijn, F.; Sie, S. T.; Moulijn, J. A.; van den Bleek, C. M. A Numerical Comparison of Alternative Three-Phase Reactors with a Conventional Trickle-Bed Reactor. The Advantages of Countercurrent Flow for Hydrodesulfurization. *Chem. Eng. Sci.* **1999**, *54*, 4791.

(13) Taylor, R.; Krishna, R. Modeling reactive distillation. *Chem. Eng. Sci.* **2000**, *55*, 5183–5229.

(14) Hidalgo-Vivas, G. P.; Towler. Distillate hydrotreatment by reactive distillation. Presented at *AIChE Annual Meeting*, Miami Beach, Nov 15–20, 1998.

(15) Plazas-Rosas, F. Application of the Concept of Distillation with Reactor Side in the Hydrodesulfurization of Diesel. Thesis for Master Degree, Universidad Autónoma Metropolitana-Iztapalapa, México, 2008.

(16) Van Parijs, I.; Froment, G. Kinetics of Hydrodesulfurization on a Cobalt-Molybdenum/ $\gamma$ -Alumina Catalyst. Part 1. Kinetics of the Hydrogenolysis of Thiophene. *Ind. Eng. Chem. Prod. Res. Dev.* **1986**, *25*, 431.

(17) Van Parijs, I.; Hosten, L.; Froment, G. Kinetics of the Hydrodesulfurization on a Cobalt-Molybdenum/ $\gamma$ -Alumina Catalyst. Part 2. Kinetics of the Hydrogenolysis of Benzothiophene. *Ind. Eng. Chem. Prod. Res. Dev.* **1986**, *25*, 437.

(18) Vanrysselberghe, V.; Gall, R.; Froment, G. Hydrodesulfurization of 4-Methylthiophene and 4,6-Dimethylthiophene on a CoMo/Al<sub>2</sub>O<sub>3</sub> Catalyst: Reaction Network and Kinetics. *Ind. Eng. Chem. Res.* **1998**, *37*, 1235.

(19) Joback, K. G.; Reid, R. C. Estimation of Pure-Component Properties from Group Contribution. *Chem. Eng. Commun.* **1987**, *57*, 233.

(20) Sharma, S.; Rangaiah, G. P. A Hybrid Multi-Objective Optimization Algorithm, 5th International Symposium on Design. *Operation and Control of Chemical Processes* **2010**, 1494–1503.

(21) Sharma, S.; Rangaiah, G. P. Multi-Objective Optimization of a Bio-Diesel Production Process. *Fuel* **2013**, *103*, 269.

(22) Bisowarno, B. H.; Tian, Y.; Tadé, M. O. Application of side reactor on ETBE reactive distillation. *Chemical Engineering Journal* **2004**, *99*, 35–43.

(23) Ma, X.; Sakanishi, K.; Isoda, T.; Mochida, I. Hydrodesulfurization Reactivities of Narrow Cut Fractions in a Gas. *Ind. Eng. Chem. Res.* **1995**, *34* (3), 748–754.

(24) Baur, R. y; Krishna, R. Distillation column with reactive pump arounds: an alternative to reactive distillation. *Catal. Today* **2003**, *79–80*, 113–123.

(25) Turton, R.; Bailie, R. C.; Whiting, W. B.; Shaeiwitz, J. A. *Analysis, Synthesis, and Design of Chemical Process*, second ed.; Prentice Hall: USA, 2004.

(26) Gadalla, M. A.; Olujic, Z.; Jansens, P. J.; Jobson, M.; Smith, R. Reducing CO<sub>2</sub> Emissions and Energy Consumption of Heat-Integrated Distillation Systems. *Environ. Sci. Technol.* **2005**, *39*, 6860.